AIAA JOURNAL
Vol. 42, No. 12, December 2004

Torus-Less Inflated Membrane Reflector with an Exact Parabolic Center

G. Greschik* and M. M. Mikulas†
University of Colorado, Boulder, Colorado 80309-0429
and
A. Palisoc‡
L'Garde, Inc., Tustin, California 92680-6487

A possible alternative to the lenticular configuration, the concept of a torus-less pressurized membrane antenna with an exact parabolic center, is introduced. For a characteristic symmetric configuration, three membrane regions are identified: the parabolic reflector center, the (wrinkled) perimeter that suspends it, and a transition zone between. Via an analysis of the pressurization kinematics, the last of the three is seen as critical. Structural economy and optimization are considered, and a design paradigm is established and demonstrated. It is also shown that there can exist mechanically sound pressurized membrane shapes for which no strain-free initial configurations correspond. The study is restricted to the pressurized membrane itself: no application-specific system integration issues are addressed.

Nomenclature

A	=	surface area
E	=	Young's modulus
f	=	focal length of parabolic cap
h	=	(total) height of pressurized structure
N	=	membrane stress resultant
R, D	=	radius, diameter of parabolic cap
R_m, D_m	=	radius, diameter of entire membrane
r, z	=	radial and axial coordinates
s	=	meridional arc length measured from the center out
t	=	membrane thickness
α	=	meridional slope angle, $= \tan^{-1}(\mathrm{d}z/\mathrm{d}r)$
ε	=	engineering strain, $= (l - l_I)/l_I$
κ	=	meridional curvature, $= \mathrm{d}\alpha/\mathrm{d}s$
κ_c	=	surface curvature in the circumferential direction $= \sin\alpha/r$
ν	=	Poisson's ratio

Subscripts

c	=	reference to circumferential direction
I	=	reference to strain-free state
m	=	reference to meridional direction

Introduction

ACCORDING to the prevailing paradigm, parabolic inflatable membrane reflectors are constructed of two membrane caps—at least one of which is parabolic—forming a lenticular enclosure. This structure is radially suspended around its perimeter,[1] often by a torus. In addition to the enclosure, the torus can also be pressurized. The topological and the consequent mechanical, design, fabrication, and deployment complexities of this structure motivated the development of the concept that is the subject of the present study.

The torus-less reflector is a one-piece membrane that pressurizes into a shape with reflector region(s). This is illustrated in Fig. 1 for a symmetric configuration. As shown, the structure has two (exactly) parabolic "caps," which are suspended by the peripheral region of the inflated membrane shell itself. In addition to completing the membrane enclosure, the periphery serves merely as support for the cap(s), which are the operational part(s) of the reflector. As a result, one goal of the structural design is to minimize the amount of material and volume needed for this support with respect to that involved in direct reflector operation (the caps). The structural overhead of the periphery is quantified in the present paper by the ratios of the surface areas and the diameters of the entire membrane to those of the two caps (A_m/A and D_m/D, where the subscript m refers to the entire membrane and no subscript is used for the caps; Fig. 1). Another shape characteristic of likely design interest is the height-to-diameter aspect ratio h_m/D_m. The lower these measures, the more efficient the design is.

However, as it is seen in the following, there is a limit to efficiency that depends on the cap geometry, the membrane stiffness, and the applied pressure. These factors define the most economic shape through the mechanics and the pressurization kinematics of the entire structure. To study these effects, two regions of the membrane outside the parabolic caps, characterized by qualitatively different behavior, must be distinguished. One is the outer region where no hoop stresses are present (this means wrinkling), the other is the transition zone between the former and the cap (Fig. 2). The transition zone, although its size might be insignificant with respect to the rest of the membrane, has a critical role in the mechanics of the whole.

To show this, relevant aspects of membrane mechanics are reviewed first. (The formulation is that incorporated in the software *AM*, which has been instrumental to the present study.) In the framework thus established, the parabolic cap and the wrinkled perimeter are discussed next. The incompatibility of the two is seen to necessitate a transition zone between. The geometric analysis of this necessity is followed by the consideration of the physical behavior of the membrane. The latter puts a lower bound on the transition zone width for any particular design problem.

A byproduct of the study is the illustration of the remarkable fact that there can exist mechanically sound pressurized membrane shapes to which no strain-free initial membrane configurations

Presented as Paper 2000-1798 at the 41st Structures, Structural Dynamics, and Materials Conference, Atlanta, GA, 3–6 April 2000; received 9 May 2002; accepted for publication 27 May 2004.

*Research Associate, C.Box 429, Center for Aerospace Structures, UCB 429; greschik@colorado.edu. Member AIAA.

†Professor Emeritus of Aerospace Engineering, C.Box 429, Center for Aerospace Structures, UCB 429; mikulas@colorado.edu. Fellow AIAA.

‡Structural Engineer, 15181 Woodlawn Avenue; art_palisoc@Lgarde.com.

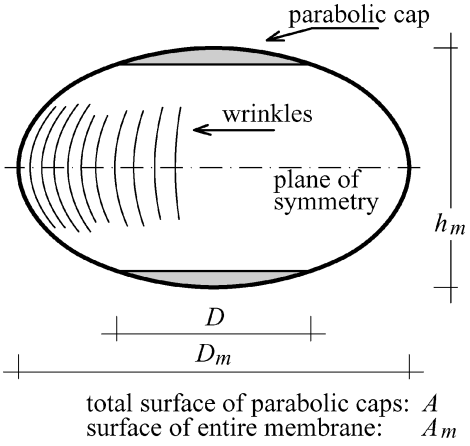

Fig. 1 Torus-less inflatable reflector.

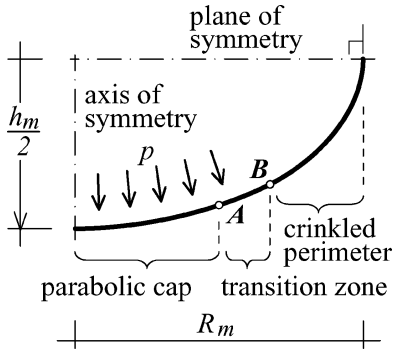

Fig. 2 Pressurized contour.

correspond. Finally, the results of a parametric study of reflector structural efficiency are discussed.

Membrane Mechanics

To back the subsequent analysis of the torus-less reflector, selected aspects of the mechanics of an axisymmetric membrane are reviewed. Of several mathematically equivalent approaches, the formulation herein adopted is that incorporated in the software package *AM* developed for the quick yet accurate analysis of axisymmetric membranes.[2,3] (*AM* has been the main tool for the present study.) The choices made during problem formulation and algorithm development reflect concerns of programming simplicity, of streamlining details for software modularity and extendibility, and of computational efficiency.

Governing Equations

Instead of directly addressing the two-dimensional membrane field equations, exploit symmetry by reducing the formulation to that of the meridian. Further, following Ref. 2, consider only one symmetric quarter of the entire oval contour (Fig. 2) and use the radial and axial coordinates r and z of a cylindrical frame of reference placed at the intersection of the structure's axis and plane of symmetry. The orientation of this coordinate system and the key geometric variables used are shown in Fig. 3 via the contour deformation from the initial state I affected by the applied pressure p.

As in Ref. 2, the geometric quantities associated with this deformation are

$$\varepsilon_c = \frac{r}{r_I} - 1 \tag{1}$$

$$\varepsilon_m = \frac{\mathrm{d}s}{\mathrm{d}s_I} - 1 \tag{2}$$

$$\kappa = \frac{\mathrm{d}\alpha}{\mathrm{d}s} \tag{3}$$

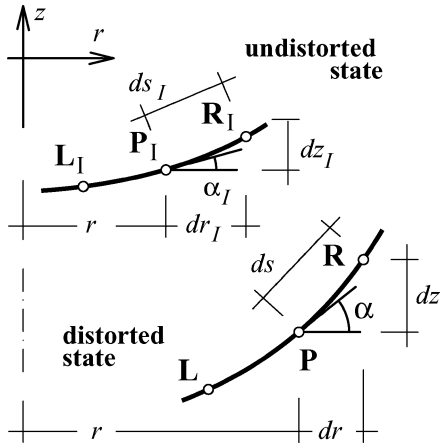

Fig. 3 Geometry of deformations.

$$\frac{\mathrm{d}r}{\mathrm{d}s} = \cos\alpha \tag{4}$$

$$\frac{\mathrm{d}z}{\mathrm{d}s} = \sin\alpha \tag{5}$$

where ε_c and ε_m are engineering strains in the circumferential and meridional directions (Fig. 3).

The axial equilibrium of a cap of the membrane defined by radius r and the equilibrium of the membrane in the surface normal direction at point $z(r)$ entail

$$pr = 2N_m \sin\alpha \tag{6}$$

$$p = N_m\kappa + N_c\kappa_c \tag{7}$$

where

$$\kappa_c = \sin\alpha/r \tag{8}$$

is the surface curvature in the circumferential direction, p is the internal pressure, and N_m and N_c are the true (Cauchy-type) radial and circumferential membrane stress resultants.

The set of governing equations is completed by the constitutive relations, which, for the presently considered case of linear elasticity and isotropy, are

$$Et\varepsilon_c = N_c(1+\varepsilon_m) - \nu N_m(1+\varepsilon_c) \tag{9}$$

$$Et\varepsilon_m = N_m(1+\varepsilon_c) - \nu N_c(1+\varepsilon_m) \tag{10}$$

where $(1+\varepsilon)$ terms translate the Cauchy-type stress resultants into first Piola–Kirchhoff-type quantities. The phrase "first Piola-Kirchhoff-type" simply refers to the fact that the stress quantities $N_m(1+\varepsilon_c)$ and $N_c(1+\varepsilon_m)$ are defined in terms of the initial stress-free, as opposed to the deformed, reference model geometry: "The first Piola-Kirchhoff stress tensor . . . gives the actual force . . . on the deformed [surface] but is reckoned per unit area of the undeformed [surface]."[4] However, instead of the actual (elements of a) classic stress tensor, merely analogous stress quantities are conveniently defined and used.

The stresses in Eqs. (9) and (10) need to be referred to the initial model state because the constitutive parameters for a linear elastic material are generally interpreted and are readily available with respect to the initial configuration only. Yet, the nature of nonlinearities in the problem considered here necessitates the rigorous distinction of initial and deformed geometries, resulting in the form of relations (9) and (10). This combination of linearity in the constitutive law and the precise and fully nonlinear treatment of geometric nonlinearities in global model kinematics results in an accurate large displacement and deformation formulation with its scope limited to small strains.

If the membrane wrinkles (in the circumferential direction, with the wrinkles meridionally aligned), then Eqs. (9) and (10) are reduced to[2]

$$N_c = 0 \tag{11}$$

$$N_m(1+\varepsilon_c) = Et\varepsilon_m \tag{12}$$

Wrinkling is recognized to occur if the full two-dimensional constitutive relations (9) and (10) associate negative stress component(s) with a particular strain pattern.

One can easily see that the wrinkled constitutive relations (11) and (12) indeed exactly reflect the material response regardless of the extent of the extra compressive strain ε_w associated with the wrinkling. For this, first observe that relation (11) obviously holds as a pressurized axisymmetric membrane can only wrinkle with the hoop stress dropping to zero. (The meridional stresses cannot disappear.) Second, consider that the meridional response, uniaxial with no interaction with the zero hoop stresses, entails

$$\sigma_{\mathrm{mI}} = E\varepsilon_m \tag{13}$$

where σ_{mI} is the skin stress referred to the initial configuration as indicated with subscript I. As skin stress is the ratio of membrane force to thickness, then

$$N_{\mathrm{mI}}/t = E\varepsilon_m \tag{14}$$

$$N_{\mathrm{mI}} = Et\varepsilon_m \tag{15}$$

from which Eq. (12) directly follows after expressing the first Piola–Kirchhoff-type membrane force quantity N_{mI} with the true N_m membrane force in the deformed state: $N_{\mathrm{mI}} = N_m(1+\varepsilon_c)$. Whereas, obviously, the full hoop strain ε_c is the combination of the Poisson strain ε_P and the extra wrinkle strain ε_w

$$\varepsilon_c = \varepsilon_m + \varepsilon_w + \varepsilon_w\varepsilon_w \tag{16}$$

this decomposition is immaterial in the context of the current formulation, and the individual components do not appear in the final formulation at all.

Second-Order Continuity

Limit attention to problems where the membrane thickness, material properties, and the pressure vary continuously along the meridian.

The governing relations (1–12) directly or indirectly involve derivatives of the contour shape of order of at most two (the curvatures κ and κ_c). Because the formulation is continuous (everywhere except at the singularity at $r=0$), an important corollary follows. In particular, if the condition of no compressive stresses is satisfied, the necessary and sufficient condition for an arbitrary contour shape to be mechanically feasible is second-order continuity.

Two comments are needed to avoid a possible misunderstanding of this statement. First, mechanical feasibility is meant in the sense of satisfying the governing equations. Consequently, one might be inclined to talk about "mathematical," instead of "mechanical," feasibility. Still, the latter term is preferred here because the governing equations are mechanical. Second, we have to highlight that the physical meaning of this mechanical feasibility means that an actual membrane with the given pressurized shape can exist. In other words, continuous variation(s) along the meridian of the membrane thickness, material properties, and/or applied pressure can be specified to produce the specified shape.

Second-order continuity mandates the continuity of κ and κ_c. If the shape is smooth, which is necessarily the case, the continuity of these variables is equivalent to that of their ratio κ/κ_c. The design process described next for the torus-less reflector relies on this observation.

Characteristic Design

The mechanics and pressurization kinematics of the three membrane regions (the parabolic cap, the wrinkled perimeter, and the transition zone) are discussed in the following in terms of the formulation just reviewed.

Parabolic Cap

The membrane center inflates to a paraboloid (from an initial shape that can be determined, for example, as described in Ref. 2). For the corresponding section of the contour, thus

$$z = \frac{r^2}{4f} + C \tag{17}$$

$$\alpha = \operatorname{atan}\left(\frac{\mathrm{d}z}{\mathrm{d}r}\right) = \operatorname{atan}\left(\frac{r}{2f}\right) \tag{18}$$

$$\kappa = \left(\frac{\mathrm{d}z^2}{\mathrm{d}^2 r}\right) \Big/ \left[1+\left(\frac{\mathrm{d}z}{\mathrm{d}r}\right)^2\right]^{1.5} = \frac{4f^2}{(4f^2+r^2)^{1.5}} \tag{19}$$

These functions, via Eqs. (6) and (7), yield uniformly positive N_m and N_c fields for any $p>0$. Hence the unwrinkled constitutive relations (9) and (10) can be used to determine the associated strains, which also prove uniformly positive:

$$\varepsilon_c, \varepsilon_m > 0 \tag{20}$$

This result, via Eq. (1), implies $r > r_I$, that is, each material point on the parabolic cap moves radially outwards during pressurization. The magnitude of this radial displacement increases from zero at the center outward.

Via Eqs. (8), (18), and (19) the ratio of meridional and circumferential curvatures is

$$\kappa/\kappa_c = 4f^2/(4f^2+r^2) \tag{21}$$

Wrinkled Perimeter

If a symmetric self-supporting membrane is contstrained to have a particular cap shape as in Fig. 1, the minimization of its overall dimensions must be achieved via varying the shape of its periphery alone. Clearly, the faster the contour "turns vertical" moving away from the center (cap), the smaller the overall enclosure. Formally, for a structurally efficient design the contour curvature κ must be maximized at every location along the contour. From Eq. (7) and the conditions $N_c >= 0$ (for any true membrane) and $\sin\alpha > 0$ (for our model), maximum κ corresponds to

$$N_c = 0 \tag{22}$$

For the enclosure to be minimal, the membrane periphery must be wrinkled (or be at the verge of wrinkling).

Condition (22) renders the relations (6) and (7) solvable for the membrane geometry to yield

$$\kappa = 2\sin\alpha/r \tag{23}$$

or, in terms of the radius of curvature $R_\kappa = 1/\kappa$,

$$R_\kappa = r/(2\sin\alpha) \tag{24}$$

This constitutes a geometric definition of the parachute curve,[5,6] one of a family of elliptic functions that describe balloon equilibrium shapes.[7]

It is educational to consider the geometric meaning of Eq. (24). Construct the normal to the parachute curve at point **P**, and let the

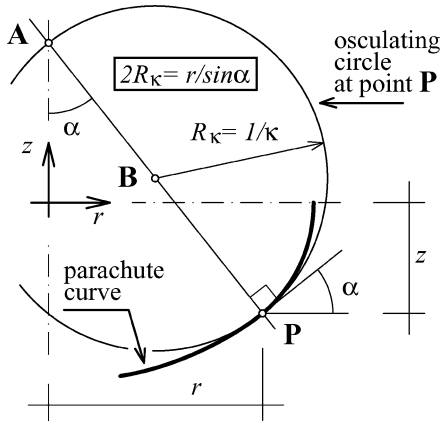

Fig. 4 Parachute curve.

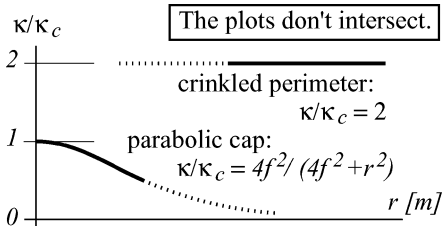

Fig. 5 Curvature ratio as a function of *r*.

intersection of this normal with the axis of symmetry z be **A** as shown in Fig. 4. (The radial distance of **P** from z is r.)

Because the vector $\boldsymbol{AP}$ subtends with z the parachute curve's α slope angle at **P**, the distance $\overline{\mathbf{AP}} = r/\sin\alpha$. This is twice the right-hand side of Eq. (24). Thus the diametrically opposite point of the parachute curve's osculating circle at **P** is on z, and the circle's center **B** is bisecting **AP**.

Note further that Eq. (23) can also be written, via Eq. (8), as

$$\kappa/\kappa_c = 2 \tag{25}$$

Because $N_m > 0$ [compare Eq. (6) and $\sin\alpha > 0$], a corollary of Eqs. (9) and (22) is that $\varepsilon_c < 0$. This implies $r < r_I$ through Eq. (1). Thus each material point on the wrinkled perimeter moves radially inward when the structure is pressurized. [Note that this reasoning is wrong if the cited Eq. (9) is no longer valid because wrinkles develop. Wrinkling, however, directly entails $\varepsilon_c < 0$ from which $r < r_I$ follows.]

Transition Zone

According to the condition of second-order continuity just described, the mechanical feasibility of a reflector contour requires that the ratio κ/κ_c of the meridional and circumferential surface curvatures be continuous. However, this continuity cannot be provided between the parabolic cap and the crinkled perimeter, as apparent from the plots of this ratio for the two regions [Eqs. (21) and (25)] shown in Fig. 5. The two regions are incompatible: second-order continuity between the two can be provided only via the presence of a third, transition, zone.

An alternative way to see the necessity of the transition zone is via the pattern of hoop strains. For the cap, circumferential strains and stresses are positive. However, these are respectively negative and zero because of wrinkling for the periphery. Clearly, a domain under finite tension cannot be directly connected to one compressively strained.

Considering the radial displacement patterns for the cap and the perimeter just discussed, the membrane's pressurization kinematics is as shown in Fig. 6. The inner and outer boundaries **A** and **B** (Fig. 2) of the transition zone radially expand and contract with the adjacent regions to accommodate the drop of the hoop stress across (from the value associated with the paraboloid shape at point **A** to zero

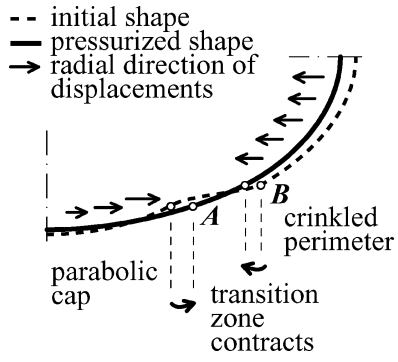

Fig. 6 Pressurization kinematics.

where crinkling begins at point **B**). The zone's width thus contracts during pressurization. In other words, the transition zone's initial configuration is radially stretched with respect to its final contour. This manifests as a wave-shaped perturbation of the initial contour as illustrated in Fig. 6 if the inflated shape is smoothly convex.

Geometric Side of Design

For the pressurized contour, the shapes of the parabolic cap and of the crinkled periphery are geometrically defined [Eqs. (17) and (24)]. Further, the condition of second-order continuity for the feasibility of a pressurized shape is also geometric. This enables the design of a pressurized contour in a purely geometric manner. One possible procedure for this is outlined in the following.

Start with the parabolic cap's shape (determined a priori from reflector operational criteria). The transition zone begins at the outermost point of this paraboloid with a contour slope and curvature of the parabola thereat for second-order continuity. The challenge of the design is to construct a (an) (optimal) transition zone starting with these constraints such that the slope and curvature, continuously varying along, finally match those on a (an) (appropriately scaled) parachute curve. From that point on, the parachute curve completes the geometry.

Algorithms to provide any of a number of such transitions can be constructed. One such scheme has been derived for the present study and implemented as a design utility to complement the software package AM^2.

Computational Algorithm

As in the finite difference method, AM and its newly developed pressurized contour design utility rely on a discrete representation of the contour at a series of points (such as **L**, **P**, and **R** in Fig. 3). The solution of a pressurized shape for a given strain-free one, the reverse, design, calculation called inverse solution, and the geometric design of the pressurized contour with the new utility all determine the appropriate meridian shapes point by point. These integration processes are aided, and their accuracies are ensured with iterative methods.

The feasibility of a newly designed pressurized contour is enforced via the condition of second-order continuity grasped via the curvature ratio κ/κ_c. When the integration from the center out passes the edge of the parabolic cap, it is this ratio that continues to steer the process until the curvature condition Eq. (25) of the parachute curve is reached (Fig. 5). In particular, a linear variation of κ/κ_c in terms of the radial coordinate r is enforced. (This means that the transition zone is made to correspond to a straight line laid across the two plots in Fig. 5. The initial and final points of this line are input into the program via the inner and outer boundary radii of the transition zone.) Once the outer edge of the transition zone is reached, the geometric definition of the parachute curve continues to drive the integration until completion.

Although the iterative techniques used to negotiate 1) the geometric conditions and 2) the proper selection of some global parameters such as the integration step size are numerically important, they are of marginal significance from the viewpoint of the present paper. Their details are, therefore, not discussed here.

Geometry vs Physical Reality

The design procedure just outlined is governed by geometry, with no explicit considerations of mechanical or material nature. This makes it simple and computationally efficient. This simplicity can be a significant advantage during preliminary design if the details of the relationship between the initial and pressurized shapes can be ignored. In these cases selected parameters (such as the amount of material needed) can be estimated from the final shape alone, which is calculated quickly.

However, certain physical and material aspects of a structure so geometrically designed can render it difficult, if not impossible, to fabricate. This is discussed in the following.

Physical Aspects of Design

The initial, strain-free, membrane shape can be calculated for a pressurized contour as discussed as the inverse solution in Ref. 2 and implemented in *AM*.

The inverse solution begins with the calculation of the stress state along the given pressurized contour from the applied pressure and the geometry via Eqs. (6) and (7). The associated strains are determined next via the appropriate (wrinkled or unwrinkled) constitutive relations. Finally, the obtained deformations are removed for each integration point along the pressurized shape, and the initial shape is integrated. However, there is nothing in this procedure that guarantees that the last step, the removal of the strains, yields an actual (integrable) shape. In other words, it is possible that a pressurized shape has no strain-free initial shape associated with it. Further, this can happen even if the pressurized shape is mechanically, materially, and geometrically sound, as turned out to be the case for a number of properly designed pressurized torus-less inflated reflectors investigated during the present study. Although the physical reality of the lack of a strain-free initial shape can be difficult to grasp in the abstract, it can be easily visualized in the context of the torus-less reflector.

Consider a pressurized torus-less membrane and the associated initial contour (Fig. 6). As already discussed, the initial configuration of the transition zone **AB** is radially stretched with respect to the pressurized state because of the radial displacements of its endpoints **A** and **B** during pressurization. The stress-free state of the transition zone is to accommodate this stretch. However, if the stretch is excessive, the distance between **A** and **B** for a particular stress-free parabolic cap and a crinkled perimeter can be greater than the arc length along the transition zone when the latter is relieved of stresses. In this case a continuous connection between the parabolic cap and the perimeter zone can be realized only at the cost of strains even if no pressure is applied. (These strains would materialize as crinkles in reality.) Clearly, no strain-free initial state exists.

The straightforward approach to the fabrication of an inflatable membrane is to produce (to shape and to assemble) it when stress and strain free. Such a procedure is not viable if there is no strain-free configuration. To impart prescribed strains to a membrane structure under fabrication might, in principle, be possible via, say, a careful control of the temperature field during the manufacturing process. Practical and financial constraints, however, can render such a procedure impossible. For the purpose of the present study, therefore, a pressurized shape with no associated strain-free configuration is deemed unacceptable. The existence of a strain-free initial shape for each design example discussed next has been verified via the inverse solver of *AM*.

Qualitative Considerations

Geometric and physical aspects of a torus-less reflector design that affect the existence of a strain-free initial state can be identified without a numerical study as well. As seen, this existence depends on the details of the pressurization kinematics. The latter, in turn, is a result of the interaction of the geometry, the pressure applied, and the membrane's material characteristics. From the kinematics of the transition zone during pressurization follows that a strain-free initial shape is more likely to exist if 1) the pressure is low, 2) the membrane is stiff, 3) the transition zone is steep (it is associated with high contour slopes), and 4) the transition zone is long. The first two effects lessen the radial stretch between the initial and pressurized states of the transition zone and the last two help the region to accommodate the stretch.

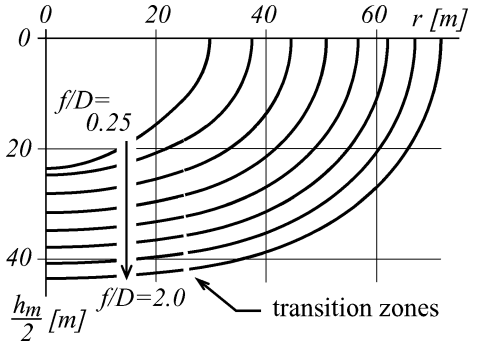

Fig. 7 Pressurized contours with minimal transition zone lengths for various cap *f/D* ratios.

However, as it will be seen in the following section, the shorter the transition zone, the more structurally efficient a design. The desirability of a long transition zone to enable a sound initial shape pointed out earlier is thus in direct conflict with what is optimal for design efficiency. This conflict can be resolved with a design paradigm according to which a minimal transition zone is sought and the pressurized shape (the transition zone steepness), the pressure, and the membrane stiffness are manipulated to make the unpressurized state acceptable.

Design Study

Selected results of a comprehensive design study of antennas up to 50-m-diam are shown in Fig. 7. The depicted contours correspond to $D = 50$-m-diam parabolic caps, with the associated f/D ratios varying from 0.25 to 2.00 with increments of 0.25. (The extremes of this range are beyond practical interest but are included in the study to better reveal trends.) The transition zone has been minimized for each contour with *AM*'s inverse solver used to verify the existence of sound initial shapes. The material properties assumed for this verification have been a membrane thickness of $t = 0.0127$ mm (half-mil), a Young's modulus of $E = 5.516$ GPa (800 ksi), and a $\nu = 0.3$ Poisson's ratio. (These constants correspond to Kapton.) A pressurization level to achieve 1.723-MPa (250-psi) skin stress at the apex has been used for each membrane. (This means a different pressure for each f/D ratio; Ref. 2.) The transition zones, marked on each contour in Fig. 7, cannot be ignored despite their relatively small dimensions with respect to those of the entire membrane. Failure to account for their presence misses a significant aspect of structural behavior. Note also that varying the parameters used in the present example (e.g., increasing the pressure or using a softer membrane material) can significantly increase transition zone sizes.

Note also that, as speculatively deduced in the preceding sections, the steeper it is, the shorter a transition zone can be. Transition zone steepness, in turn, increases with a decreasing parabolic cap f/D ratio.

The weight and dimensional efficiencies of the designs are illustrated in Fig. 8a via the ratios of the surface and diameter of the entire membrane to those of the (two) parabolic caps (compare to Fig. 1). (Note that for the canopy of a lenticular reflector such as the Inflatable Antenna Experiment (IAE)[8] both ratios are unity $A_m/A = D_m/D = 1$.) The aspect ratios of the shapes are shown in Fig. 8b. The values plotted are also listed in Table 1.

The following observations are supported by the contours shown, some additional studies not detailed herein, and geometric and mechanical considerations (compare to the preceding):

1) For a given parabolic cap geometry, the shorter the transition zone is the smaller the canopy diameter and the more weight and dimensionally efficient the design.

2) The transition zone cannot be shorter than a limit defined by the existence of a stress-free initial membrane shape.

Table 1 Efficiency and aspect ratios plotted in Figs. 8a and 8b

f/D	D_m/D	A_m/A	h_m/D_m
0.25	1.19	1.91	0.793
0.50	1.50	3.34	0.662
0.75	1.78	4.86	0.632
1.00	2.04	6.42	0.620
1.25	2.27	8.00	0.614
1.50	2.48	9.61	0.611
1.75	2.68	11.23	0.608
2.00	2.87	12.87	0.607

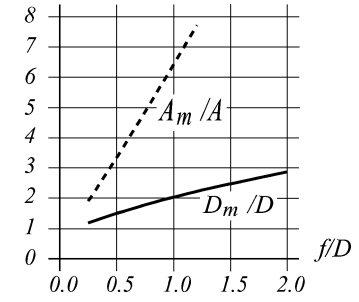

a) Efficiency ratios

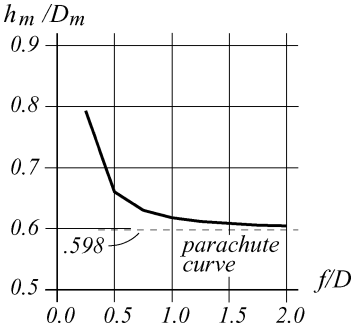

b) Contour aspect ratios

Fig. 8 Some design characteristics as functions of the parabolic cap shape.

3) The only geometric aspect of the contour design that affects the minimal transition zone length is the shape (f/D ratio) of the parabolic cap. The deeper the cap is, the shorter the transition zone can be.

4) The physical parameters that affect the transition zone length are the applied pressure and the membrane stiffness. The stiffer the membrane and the lower the pressure is, the shorter the transition zone can be.

5) The weight and dimensional efficiency of optimal designs strongly depends on the shape of the parabolic cap. Deeper caps allow more efficient shapes. For a cap f/D ratio of 0.5, the weight efficiency is $A_m/A \approx 3.4$, and the radial dimensional efficiency is $D_m/D \approx 1.5$ for the example material and load considered.

6) The weight and dimensional efficiency of optimal designs depends on the width of the transition zone only mildly. Therefore, the impact of the factors influencing the extent of the transition zone is also limited.

7) The depth-to-radius ratio of the canopy (h_m/D_m; Fig. 1) is greater than that for the parachute curve $h_m/D_m > 0.598$, and it is approaching this limit for shallow parabolic caps.

Clearly, deep parabolic caps generally perform better than shallow ones.

Conclusions

The concept of torus-less inflated membrane reflectors has been introduced, and an analysis and design methodology for this class of structures has been developed, reviewed, and illustrated via a simple but comprehensive design study. Observations regarding the feasibility of some design options have been made, and associated structural efficiencies have been assessed.

The mechanics of the torus-less inflated reflector requires three distinct structural zones to exist: a parabolic cap at the center, a crinkled perimeter, and a transition zone between. The shape of the parabolic cap defines the overall design geometry. The design challenge is to construct an optimal acceptable transition zone. The shorter the contour of this region, the more weight and shape efficient the structure. The transition contour, however, cannot be shorter than a limit defined by the existence of a strain-free initial shape for the membrane. Generally, this limit is lower for deeper parabolic caps (lower f/D ratios), lower pressures, and stiffer membranes. Most noteworthy of these observations is the first, which means that the efficiency of a design can be greatly increased if the parabolic cap is deep.

The weight efficiencies of practicable torus-less designs might or might not be worse than for lenticular, IAE-type inflated reflectors. The application of one or these reflector types for a particular project has to be carefully weighed.

A remarkable discovery made is that it is possible that a mechanically, materially, and geometrically sound pressurized membrane has no strain-free initial shape associated with it. This possibility has direct practical relevance, as the performed design study attests.

The newest version of the software package *AM*, which has been developed in Ref. 2 has been used for all analyses performed. Particularly useful has been *AM*'s inverse solver, which computes the initial shape for any—numerically or analytically given—pressurized shape. Additional design and analysis utility programs have also been written and used for the study.

Acknowledgments

The concept of the torus-less membrane reflector was innovated by L'Garde, Inc. The present work was in support by L'Garde and was sponsored by the NASA Jet Propulsion Laboratory (JPL). Technical direction and management was provided by Bob Freeland of JPL.

References

[1]Freeland, R. E., Bilyeu, G., Veal, G. R., and Mikulas, M. M., "Inflatable Deployable Space Structures Technology Summary," International Astronautical Federation, Paper 98-1.5.01, Sept.–Oct. 1998.

[2]Greschik, G., Palisoc, A., Veal, G., Cassapakis, C., and Mikulas, M. M., "Approximating Paraboloids with Axisymmetric Pressurized Membranes," AIAA Paper 98-2102, April 1998.

[3]Greschik, G., Palisoc, A., Cassapakis, C., Veal, G., and Mikulas, M. M., "Sensitivity Study of Precision Membrane Reflector Deformations," *AIAA Journal*, Vol. 39, No. 2, 2001, pp. 308–314.

[4]Malvern, L. E., *Introduction to the Mechanics of a Continuous Medium*, Prentice-Hall, Upper Saddle River, NJ, 1969, p. 222.

[5]Mikulas, M. M., "Behavior of Double Curved Partly Wrinkled Membrane Structures Formed from an Initially Flat Membrane," Ph.D. Dissertation, Virginia Polytechnic Inst. and State Univ., Blacksburg, VA, 1970.

[6]Sir Taylor, G. I., "On the Shapes of Parachutes," *The Scientific Papers of Sir G. I. Taylor*, edited by G. K. Batchelor, Vol. 3, Cambridge Univ. Press, 1963, pp. 26–37.

[7]Baginski, F., Collier, W., and Williams, T., "A Parallel Shooting Method for Determining the Natural Shape of a Large Scientific Balloon," *SIAM Journal on Applied Mathematics*, Vol. 58, No. 3, 1998, pp. 961–974.

[8]Freeland, R. E., and Bilyeu, G., "IN-STEP Inflatable Antenna Experiment," International Astronautical Federation, Paper 92-0301, Aug.–Sept. 1992.

E. Livne
Associate Editor